NASA Contractor Report 198418
ICOMP–95–21; CMOTT–95–4

Calculations of Diffuser Flows With an Anisotropic K-ε Model

J. Zhu and T.-H. Shih
Institute for Computational Mechanics in Propulsion
and Center for Modeling of Turbulence and Transition
Lewis Research Center
Cleveland, Ohio

November 1995

Prepared for
Lewis Research Center
Under Cooperative Agreement NCC3–370

National Aeronautics and
Space Administration

Calculations of Diffuser Flows with an Anisotropic K-ϵ Model

J. Zhu and T.-H. Shih
Center for Modeling of Turbulence and Transition
ICOMP, OAI, NASA Lewis Research Center
Cleveland, OH 44135

ABSTRACT

A newly developed anisotropic K-ϵ model is applied to calculate three axisymmetric diffuser flows with or without separation. The new model uses a quadratic stress-strain relation and satisfies the realizability conditions, i.e., it ensures both the positivity of the turbulent normal stresses and the Schwarz' inequality between any fluctuating velocities. Calculations are carried out with a finite-volume method. A second-order accurate, bounded convection scheme and sufficiently fine grids are used to ensure numerical credibility of the solutions. The standard K-ϵ model is also used in order to highlight the performance of the new model. Comparison with the experimental data shows that the anisotropic K-ϵ model performs consistently better than does the standard K-ϵ model in all of the three test cases.

1. INTRODUCTION

Diffusers are widely used in aeropropulsion systems such as engine inlet, nozzle and combustion chamber. The maneuverability of modern aircraft at a wide range of speeds requires to control engine face flow distortion. Flow recirculation in combustors is critical to stabilize flames and to increase the fuel mixing efficiency. Therefore, the understanding of diffuser flows is of paramount importance to the design of such devices. Until recently, calculations of diffuser flows in the aeropropulsion community have been almost done with either mixing-length models such as the Baldwin-Lomax model or two-equation isotropic eddy viscosity models. The computational results are often less than satisfactory for the purpose of design, and this is mainly attributed to turbulence modeling. The limitations of the mixing-length models are quite apparent, and it is questionable whether improvements in predicting general diffuser flows can be made using this kind of models. Two-equation isotropic eddy viscosity models also have some undesirable features such as isotropy and poor response to both adverse pressure gradient and streamline curvature effects.

Recently, Shih and Lumley (1993) have developed a sixth-order stress-strain relation under the assumption that the turbulent stress is a function of the mean deformation tensor, the velocity and length scales of turbulence characterized by the turbulent kinetic energy and its dissipation rate. This is the most general constitutive relation for the Reynolds stress within the framework of algebraic turbulence modeling, with the linear stress-strain relation in the Boussinesq's eddy-viscosity concept being its first-order approximation. The general relation contains eleven coefficients to be determined, an inconvenience for practical applications. Therefore, Shih et al. (1994) have developed

a new anisotropic K-ϵ model which uses a truncated quadratic stress-strain relation in conjunction with the two modeled transport equations for the turbulent kinetic energy and its dissipation rate. The new model has the following desirable features: (a) it is fully realizable, i.e., it ensures both the positivity of the turbulent normal stresses and the Schwarz' inequality for turbulent shear stresses; (b) it accounts for the effect of the mean deformation rate by which the eddy-viscosity will be maintained at an adequate level to mimic complex flow structures; (c) it shows the proper lack of a rotation effect on the isotropic turbulence, satisfying the rapid distortion theory; and (d) it is easier to use, as compared to other formulations. Simplicity is of great value for practical engineering applications. The model were calibrated using both well-studied basic flows (e.g. homogenous shear flows and the surface flows in the inertial sublayer) and complicated backward-facing step flows.

In this work, the new anisotropic K-ϵ model is applied to calculate three axisymmetric diffuser flows, two attached and one separated, all of which undergo strong adverse pressure gradients. The standard K-ϵ model (Launder and Spalding, 1974) is also used, since it is the most popular turbulence model used today in calculations of complicated flows and can also be used to highlight the performance of the new model. The calculations are carried out with a finite-volume method. The numerical accuracy of solutions is ensured by using a second-order accurate, bounded convection scheme and sufficiently fine grids. The performances of the models are examined through extensive comparisons with experimental data.

2. CALCULATION PROCEDURE

Incompressible, steady-state, turbulent flows are governed by the following Reynolds averaged continuity and Navier-Stokes equations:

$$U_{i,i} = 0 \tag{1}$$

$$(\rho U_j U_i - \mu U_{i,j} - \tau_{ij})_{,j} = -p_{,i} \tag{2}$$

where U_i is the mean velocity component in x_i-direction, p is the pressure, μ and ρ are the fluid molecular viscosity and density, and $U_{i,j}$ is the derivative of U_i with respect to the co-ordinate x_j, respectively. The Reynolds stress $\tau_{ij}(= -\rho\overline{u_i u_j})$ in Eq.(2) is calculated by using the following two turbulence models:

1) Standard K-ϵ model

$$\tau_{ij} = \mu_t(U_{i,j} + U_{j,i}) - \frac{2}{3}\rho K \delta_{ij} \tag{3}$$

$$\mu_t = C_\mu \rho K^2/\epsilon \tag{4}$$

$$[\rho U_j K - (\mu + \frac{\mu_t}{\sigma_K})K_{,j}]_{,j} = \tau_{ij}U_{i,j} - \rho\epsilon \tag{5}$$

$$[\rho U_j \epsilon - (\mu + \frac{\mu_t}{\sigma_\epsilon})\epsilon_{,j}]_{,j} = C_{1\epsilon}\tau_{ij}U_{i,j}\frac{\epsilon}{K} - C_{2\epsilon}\rho\frac{\epsilon^2}{K} \tag{6}$$

$$C_\mu = 0.09,\ C_{1\epsilon} = 1.44,\ C_{2\epsilon} = 1.92,\ \sigma_K = 1,\ \sigma_\epsilon = 1.3 \tag{7}$$

2) Anisotropic K-ϵ model

$$\tau_{ij} = -\frac{2}{3}\rho K\delta_{ij} + 2\mu_t S_{ij} + 2C_2\rho\frac{K^3}{\epsilon^2}(S_{ik}\Omega_{kj} - \Omega_{ik}S_{kj}) \tag{8}$$

where

$$\mu_t = C_\mu \rho K^2/\epsilon, \quad C_\mu = 1/(6.5 + A_s U^* K/\epsilon) \tag{9}$$

$$C_2 = \frac{\sqrt{1 - 9(C_\mu SK/\epsilon)^2}}{1 + 6(SK/\epsilon)(\Omega K/\epsilon)} \tag{10}$$

$$A_s = \sqrt{6}\cos\phi \tag{11}$$

$$\phi = \frac{1}{3}arc\cos(\sqrt{6}W) \tag{12}$$

$$W = \frac{S_{ij}S_{jk}S_{ki}}{S^3} \tag{13}$$

$$U^* = \sqrt{S_{ij}S_{ij} + \Omega_{ij}\Omega_{ij}} \tag{14}$$

$$S = \sqrt{S_{ij}S_{ij}} \tag{15}$$

$$S_{ij} = \frac{1}{2}(U_{i,j} + U_{j,i}) \tag{16}$$

$$\Omega_{ij} = \frac{1}{2}(U_{i,j} - U_{j,i}) \tag{17}$$

The K and ϵ in the anisotropic K-ϵ model are calculated with the same equations as in the standard K-ϵ model.

The above two models are of high Reynolds number form, therefore, they cannot be integrated down to the wall. In this work, the standard wall function approach (Launder and Spalding, 1974) is used to bridge the near-wall region.

Numerical calculations are carried out by using a conservative finite-volume method designed for calculating two-dimensional planar or axisymmetric, incompressible, elliptic flows with complex boundaries. The method uses a non-staggered variable arrangement, namely, all the dependent variables are stored at the geometric center of each control volume. The momentum interpolation of Rhie and Chow (1983) is used to avoid checkerboard oscillations usually associated with non-staggered grids. The velocity-pressure coupling is achieved via the SIMPLEC algorithm (Van Doormal and Raithby, 1984). Numerical implementation of the anisotropic K-ϵ model is straightforward; the linear part in Eq.(8) is treated in the same manner as in the standard K-ϵ model and the quadratic part is included in the source terms. To ensure numerical accuracy and stability, the convection terms of all the transport equations are differenced by the hybrid linear/parabolic approximation (HLPA) of second-order accuracy (Zhu, 1991a), and all the other terms by the conventional central differencing scheme. The resulting set of algebraic difference

equations is solved with the strongly implicit procedure of Stone (1968). The details of the present numerical procedure are given in Rodi et al. (1989) and Zhu (1991b).

3. RESULTS

All calculations were performed on the Cray YMP computer. Grid sensitivity tests were conducted using different grids ranging from 51×41 to 161×100, and the results to be presented in the following are all grid-independent. The length of computational domain was taken as 20Ro with Ro being the radius of the diffuser at entrance.

3.1 Azad and Kassab's case

The experimental apparatus of Azad and Kassab (1989) was a long pipe followed by the diffuser with an 8^o included angle. The Reynolds number based on the diameter of the pipe and the bulk mean velocity in the pipe was 1.15×10^5 and the fully developed flow conditions were at the entry of the diffuser. The calculations were made using a 83×53 grid. The first grid point away from the duct wall had the value of y^+ varying between $36 \sim 67$. At the inlet of the diffuser, the fully developed flow conditions were specified which were obtained from a separate calculation of the flow in a long pipe. The iterations and CPU-time in seconds required to get the maximum normalized residue of all the dependent variables below 10^{-6} were 546 and 74 for the anisotropic K-ϵ (AKE) model, 499 and 64 for the standard K-ϵ (SKE) model.

Figures 1 and 2 show the axial variations of calculated and measured wall static pressure coefficient and centerline velocity. It is seen that the results of the AKE model are in good agreement with the experimental data along almost the entire length of the diffuser, while the SKE model overpredicts the pressure coefficient and underpredicts the centerline velocity decay in the downstream region of the diffuser. Figures 3 and 4 show the profiles of turbulent kinetic energy and shear stress at three axial positions; here both the turbulent kinetic energy and shear stress are normilized by the bulk mean velocity in the pipe. Although the agreement with the experimental data is less satisfactory in figures 3 and 4 for the turbulent quantities than in figures 1 and 2 for the mean flow quantities, the AKE model is still seen to performs better than does the SKE model in predicting the turbulent quantities, overall.

3.2 Fraser's case

The diffuser in the experiment of Fraser (1958) had a 10^o included angle, and the Reynolds number based on the inlet diameter and the free stream velocity was 5.08×10^5. This flow was also a test case for the 1968 AFOSR-IFP-Stanford Conference (Coles and Hirst, 1968). Unlike the Azad and Kassab's case, the Fraser's flow was of boundary layer type. The computational domain was discretized by a 145×52 grid. No turbulent data was available and it has been found that inlet turbulent boundary conditions had a big influence on the computed results. In this study, these boundary conditions were obtained from the outlet profiles of a pipe flow, calculated separately and by try and error so that the flow velocity at the pipe outlet matched the experimental data at the inlet of the diffuser.

Figures 5 and 6 show the friction coefficient and the static pressure coefficient along the duct wall. Figures 7 to 9 show three boundary layer quantities, i.e., the displacement thickness, momentum thickness and shape factor. Figure 10 shows the centerline velocity decay and figure 11 shows the axial mean velocity profiles at three axial positions. It can be seen from all these figures that the results of the AKE model are consistently better

than those of the SKE model, especially at downstream locations.

3.3 Binder and Kian's case

The flow configuration of the confined jet, measured by Binder and Kian (1983), is sketched in figure 12. The diffuser has a half angle $\theta = 2.5°$ and the inlet diameter $D_o = 16$cm. At the entrance, two uniform flows, a jet of larger velocity U_J from the nozzle of diameter $d_o = 1.6$cm and an ambient stream of smaller velocity U_a, are discharged into the diffuser. The inlet flow conditions can be characterized by the Craya-Curtet number C_t and the experiment showed that recirculation occurs when $C_t < 1.10$. Several C_t values were considered in the experiment, but in the present study, only the flow at $C_t = 0.59$ was calculated, which corresponded to $U_J = 40$cm/s and $U_a = 2.33$cm/s. Under this condition, the flow had a strong separation and the previous calculations gave the worst agreement with the measurement (Zhu, 1986). A 86×50 grid was used in this calculation.

Figure 13 shows the variation of pressure coefficients along the duct wall. Here, C_p is defined by

$$C_p = \frac{\Delta p - \rho U_a^2/2}{\rho U_J^2/2} \tag{18}$$

and Δp is the pressure difference between the location x and the entrance. The pressure variation is governed by the jet entrainment, the contraction and expansion of the flow caused by recirculation bubble as well as the geometry of the duct. It can be shown that the entrainment and the divergence of the duct can only produce a maximum pressure difference equal to $\rho U_a^2/2$, while the pressure rise in the recirculation zone depends on the width of the recirculation bubble and can be much larger than $\rho U_a^2/2$. Regarding the comparison between predictions and experiments, it is seen that both models give good agreement with the experiment in the upstream region. However, in this region, the pressure gradient is mainly determined by the ambient potential flow on which the turbulence models have little effect. In the downstream region where recirculation occurs, the AKE result is still in good agreement with the experiment, while the SKE model predicts a premature pressure rise.

Figures 14 and 15 show the profiles of axial mean velocity and turbulent shear stress at three axial positions; here U_m and U_o are the sectional average velocity and centerline velocity, respectively. For the velocity profiles shown in figure 14, the comparison between the predictions and experiment is generally good, but both models fail to capture some detailed flow features. At the location $x/D_o = 1.25$, the experimental profile shows no constant ambient velocity portion while the calculated profiles by both models still have a vertical plateau above $r/R = 0.5$. The comparison at the location $x/D_o = 2.5$ indicates that the width of the predicted reverse-flow region is too thin and the predicted negative velocity is too small. For the turbulent shear stress shown in figure 15, the results of the ASE model are clearly better than those of the SKE model for all the locations considered. The large discrepancy seen at $x/D_o = 2.5$ is partially due to the underprediction of the width of the backflow region and partially due to the experimental uncertainty, as evidenced by the fact that in the experimental data, the change in sign of the shear stress profile occurs much further away from the duct wall than the velocity minimum.

4. CONCLUSIONS

The newly developed anisotropic K-ϵ model has been applied to calculate three conical diffuser flows. The comparisons with the experimental data show that the performance

of the new model is consistently better than that of the standard K-ϵ model in all of the three flow cases. Success of the new model resides in its nonlinear stress-strain relation and the eddy viscosity formulation which accounts for the effect of mean shear rates. The new model reduces the eddy viscosity in the region of large mean strain rates where the standard K-ϵ model always tends to result in overprediction. The calculations also indicate that the new model is as robust as the standard K-ϵ model and requires no significant increase in computing time.

REFERENCES

Azad, R.S. and Kassab, S.Z., 1989, "Turbulent flow in a conical diffuser: Overview and implications," *Phys. Fluids A*, Vol.1, No.3, pp.564-573.

Binder, G., and Kian, K., 1983, "Confined jets in a diverging duct," *Proceedings, Turbulent Shear Flows 4*, Karlsruhe, pp.7.18-7.23.

Coles, D.E. and Hirst, E.A. (editors), 1968, *Proceedings, Computation of turbulent boundary layers*, Vol.2, Compiled Data, AFOSR-IFP-Stanford Conference, California, pp.451-465.

Fraser, H.R., 1958, "The turbulent boundary layer in a conical diffuser," *J. Hydraulics Division*, pp.1684.1-1684.17.

Launder, B.E., and Spalding, D.B., 1974, "The numerical computation of turbulent flows," *Comput. Methods Appl. Mech. Engrg.*, Vol.3, pp.269-289.

Rhie, C.M., and Chow, W.L., 1983, "A numerical study of the turbulent flow past an isolated airfoil with trailing edge separation," *AIAA J.*, Vol.21, pp.1525-1532.

Rodi, W., Majumdar, S., and Schönung, B., 1989, "Finite-volume method for two-dimensional incompressible flows with complex boundaries," *Comput. Methods Appl. Mech. Engrg.*, Vol.75, pp.369-392.

Shih, T.-H., and Lumley, J.L., 1993, "Remarks on turbulent constitutive relations," NASA TM 106116.

Shih, T.-H., Zhu, J., and Lumley, J.L., 1994, "A new Reynolds stress algebraic equation model," NASA TM 106644.

Stone, H.L., 1968, "Iterative solution of implicit approximations of multidimensional partial differential equations," *SIAM J. Num. Anal.*, Vol.5, pp.530-558.

Van Doormal, J.P., and Raithby, G.D., 1984, "Enhancements of the SIMPLE method for predicting incompressible fluid flows," *Numer. Heat Transfer*, Vol.7, pp.147-163.

Zhu, J., 1986, "Calcul des jets turbulents confinés avec recirculation," Doctoral dissertation, l'Institut National Polytechnique de Grenoble, France.

Zhu, J., 1991a, "A low diffusive and oscillation-free convection scheme", *Communications in Applied Numerical Methods.*, Vol.7, pp.225-232.

Zhu, J., 1991b, "FAST-2D: A computer program for numerical simulation of two-dimensional incompressible flows with complex boundaries," Rept. No.690, Institute for Hydromechanics, University of Karlsruhe.

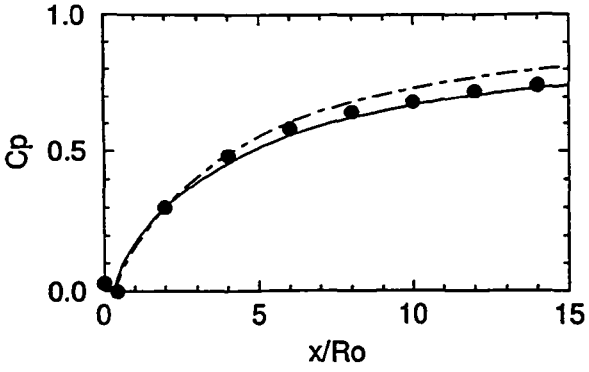

Figure 1. Pressure coefficient
—— AKE, - - - SKE, • Experiment

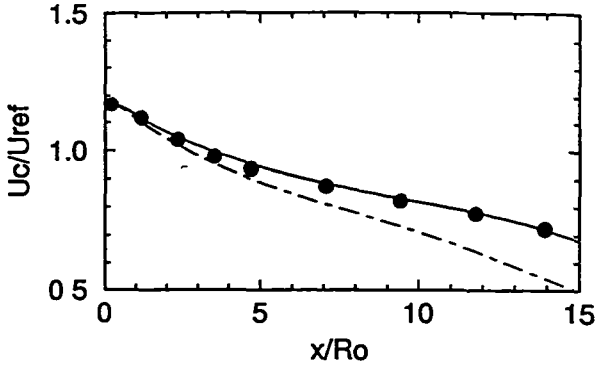

Figure 2. Centerline velocity
—— AKE, - - - SKE, • Experiment

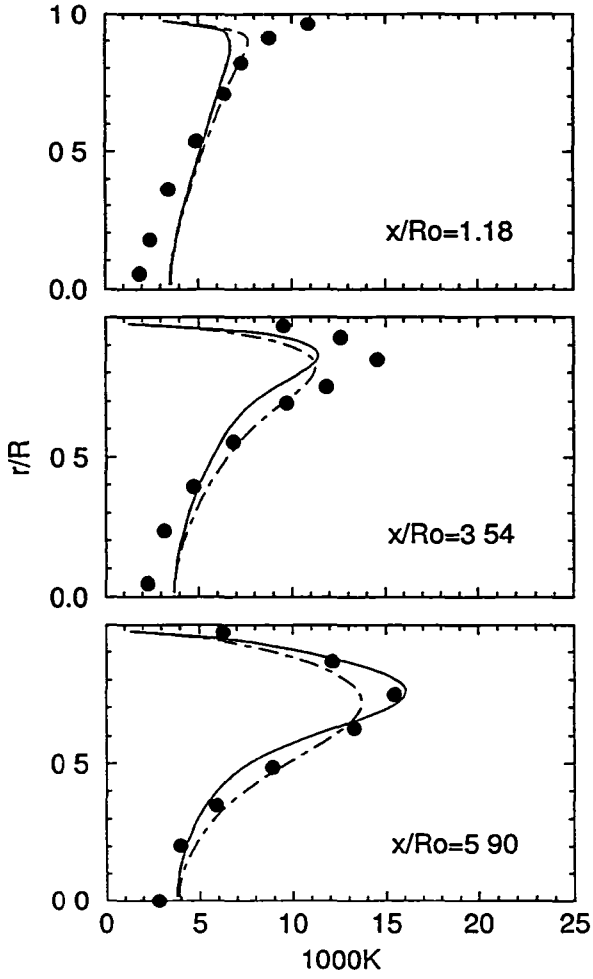

Figure 3. Turbulent kinetic energy
—— AKE, - - - SKE, • Experiment

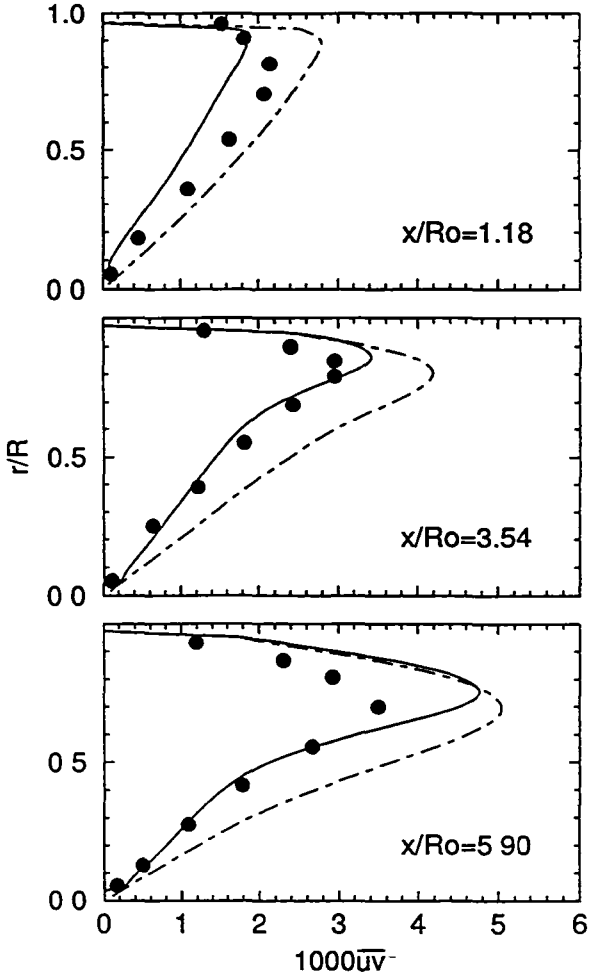

Figure 4. Turbulent shear stress
—— AKE, - - - SKE, • Experiment

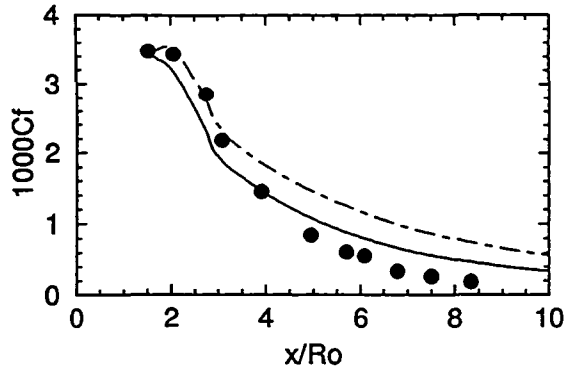

Figure 5. Wall friction coefficient
— AKE, - - - SKE, • Experiment

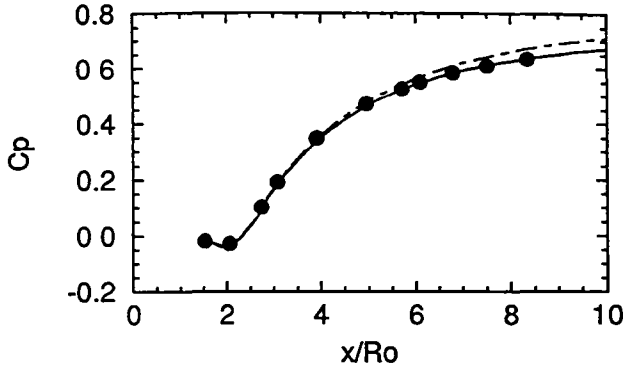

Figure 6. Pressure coefficient
— AKE, - - - SKE, • Experiment

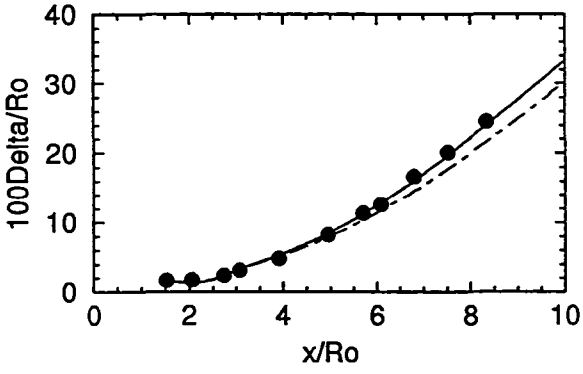

Figure 7. Displacement thickness
— AKE, - - - SKE, • Experiment

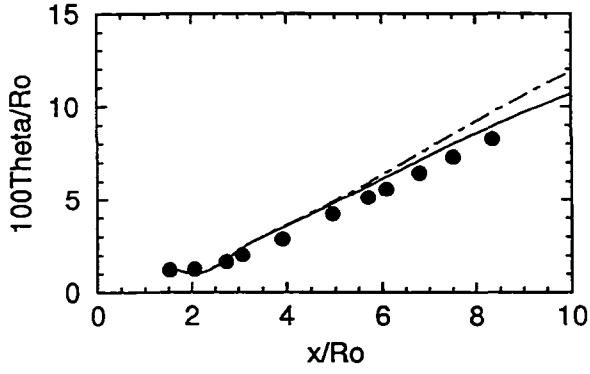

Figure 8. Momentum thickness
— AKE, - - - SKE, • Experiment

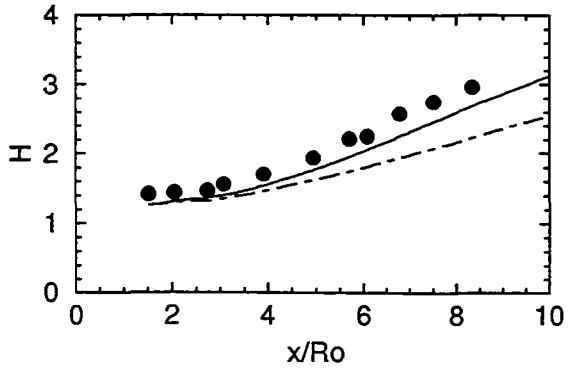

Figure 9. Shape factor
— AKE, - - - SKE, • Experiment

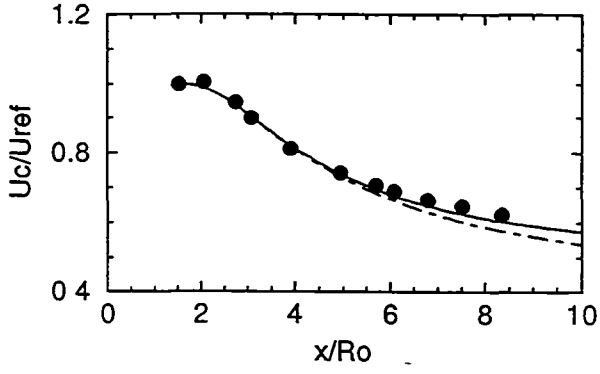

Figure 10. Centerline velocity
— AKE, - - - SKE, • Experiment

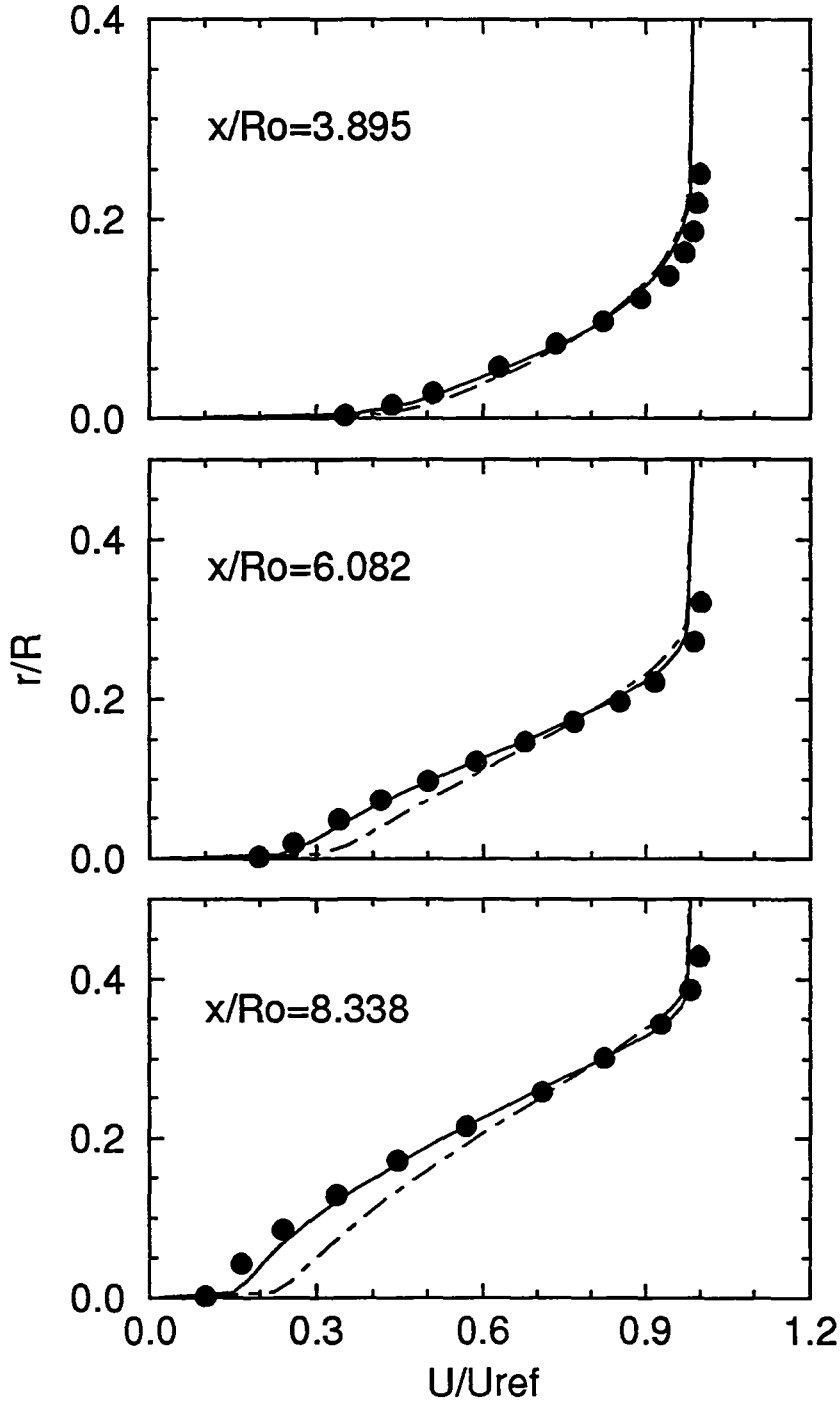

Figure 11. Axial mean velocity
— AKE, - - - SKE, • Experiment

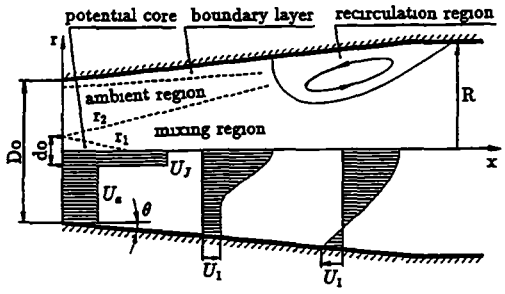

Figure 12. Flow configuration

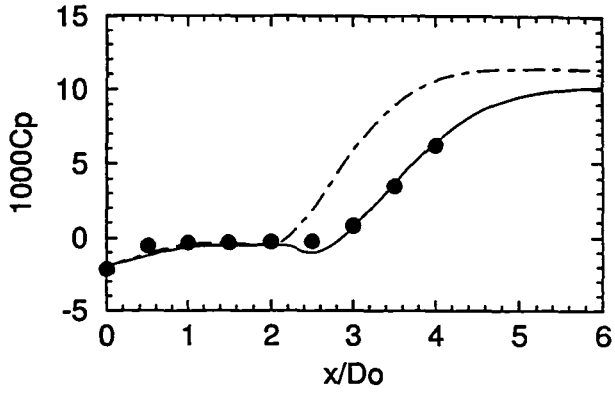

Figure 13. Pressure coefficient
— AKE, - - - SKE, • Experiment

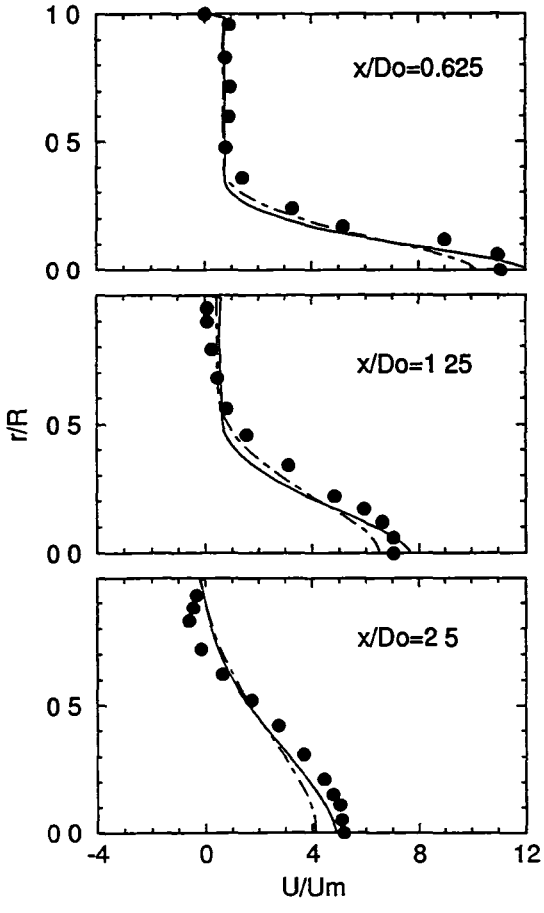

Figure 14. Axial mean velocity
— AKE, - - - SKE, • Experiment

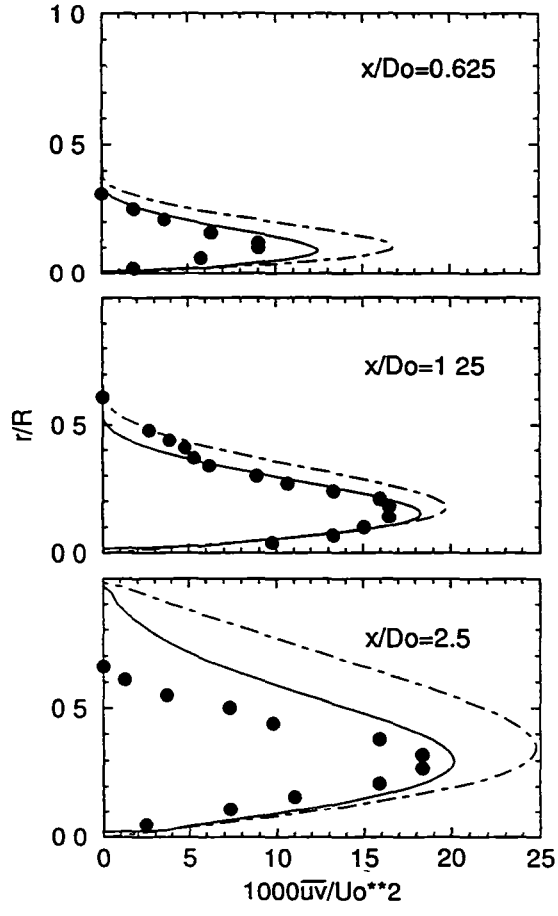

Figure 15. Turbulent shear stress
— AKE, - - - SKE, • Experiment

REPORT DOCUMENTATION PAGE

Form Approved
OMB No 0704-0188

1. AGENCY USE ONLY (*Leave blank*)	2. REPORT DATE	3. REPORT TYPE AND DATES COVERED
	October 1995	Contractor Report

4. TITLE AND SUBTITLE

Calculations of Diffuser Flows With an Anisotropic K-ε Model

5. FUNDING NUMBERS

WU-505-90-5K
NCC3-370

6. AUTHOR(S)

J. Zhu and T.-H. Shih

7. PERFORMING ORGANIZATION NAME(S) AND ADDRESS(ES)

Institute for Computational Mechanics in Propulsion
22800 Cedar Point Road
Cleveland, Ohio 44142

8. PERFORMING ORGANIZATION REPORT NUMBER

E-9988

9. SPONSORING/MONITORING AGENCY NAME(S) AND ADDRESS(ES)

National Aeronautics and Space Administration
Lewis Research Center
Cleveland, Ohio 44135-3191

10. SPONSORING/MONITORING AGENCY REPORT NUMBER

NASA CR-198418
ICOMP-95-21
CMOTT-95-4

11. SUPPLEMENTARY NOTES

Prepared for the 3rd International Symposium on Engineering Turbulence Modeling and Measurements, Crete, Greece, May 27-29, 1996. J Zhu and T-H. Shih, Institute for Computational Mechanics in Propulsion and Center for Modeling of Turbulence and Transition, NASA Lewis Research Center ICOMP Program Director, Louis A Povinelli, organization code 2600, (216) 433-5818

12a. DISTRIBUTION/AVAILABILITY STATEMENT

Unclassified - Unlimited
Subject Category 34

This publication is available from the NASA Center for Aerospace Information, (301) 621-0390

12b. DISTRIBUTION CODE

13. ABSTRACT (*Maximum 200 words*)

A newly developed anisotropic K-ε model is applied to calculate three axisymmetric diffuser flows with or without separation. The new model uses a quadratic stress-strain relation and satisfies the realizability conditions, i.e., it ensures both the positivity of the turbulent normal stresses and the Schwarz' inequality between any fluctuating velocities Calculations are carried out with a finite-volume method. A second-order accurate, bounded convection scheme and sufficiently fine grids are used to ensure numerical credibility of the solutions. The standard K-ε model is also used in order to highlight the performance of the new model. Comparison with the experimental data shows that the anisotropic K-ε model performs consistently better than does the standard K-ε model in all of the three test cases.

14. SUBJECT TERMS	15 NUMBER OF PAGES
Turbulence model; Internal flow; Incompressible flow	12
	16. PRICE CODE A03

17. SECURITY CLASSIFICATION OF REPORT	18 SECURITY CLASSIFICATION OF THIS PAGE	19 SECURITY CLASSIFICATION OF ABSTRACT	20. LIMITATION OF ABSTRACT
Unclassified	Unclassified	Unclassified	

End of Document